

Injections of Insulin in Pig Tissue Visualized by μ CT

Maria THOMSEN^{*(1)}, Mette POULSEN⁽²⁾, Bente EYVING⁽²⁾, Robert FEIDENHANS'L⁽¹⁾

(1)Nano Science Center, Niels Bohr, University of Copenhagen
Universitetsparken 5, 2100 København Ø

(2)Materials & Device Characterization (487), Novo Nordisk A/S, Hillerød.
Brennum Park 20, 3400 Hillerød

Abstract. Diabetics lack the ability to produce or use the hormone insulin sufficient and therefore they can not make completely use of glucose from the food. Subcutaneous injections of insulin are in most cases a part of their treatment and for some patients the injections are life necessary. The patients experience large fluctuations in the effect of the insulin injections, which can lead to unexpected Hypoglycemia.[1]. We have shown that by adding a contrast agent to the insulin it is possible to visualize the 3 dimensional structure of the depot in subcutis on micrometer scale by using x-rays absorption tomography. The reconstructions can give information about where the injection depot is placed in the tissue and the volume distribution of contrast agent. The diffusion of the contrast agents in dead pork tissue has been monitored over 5 hours with a time resolution of 44 sec

*mariath@fys.ku.dk

Introduction

In 2010 was the number of diabetic estimated to 151 million World Wide and the number will increase to around 366 people cording to WHO [2]. Diabetic is related to the hormone insulin which is released from the pancreas to the blood as a response of a high level of glucose in the blood. Insulin stimulates the uptake of glucose by the cells. If glucose is not taken up by the cells it causes the patients to lose in weight and get sugary urine since the cells use fatty acids as fuel instead of glucose. Diabetic patients can be divided in two groups, type 1 and type 2. Type 1 diabetes is caused by a congenital disease where the β -cells in the pancreas are destroyed. The β -cells are responsible for the production of insulin in the pancreas. Type 2 diabetics have a reduced production and response of insulin by the cells. For both type 1 and type 2 diabetic patients subcutaneous injections is a part of their treatment [1].

1. Skin structure and subcutaneous injections

Insulin is injected in subcutis which is the fat layer beneath the skin, shown schematically in figure 1a. The skin consist of 3 layers; epidermis, dermis and subcutis. The outermost layer epidermis acts as a protection of the body from infections and is separated from dermis by a membrane of connective tissue. In dermis the sweat glands and hair follicles are placed. The thickness of dermis and epidermis is around 2 mm depending on the anatomic region. Subcutis has the function of energy storage and isolating layer. It consists

of adipose tissue, which is a composition of small fat cells. These groups of fat cells are connected by interstitial tissue, a network of collagen elastic fibres [3].

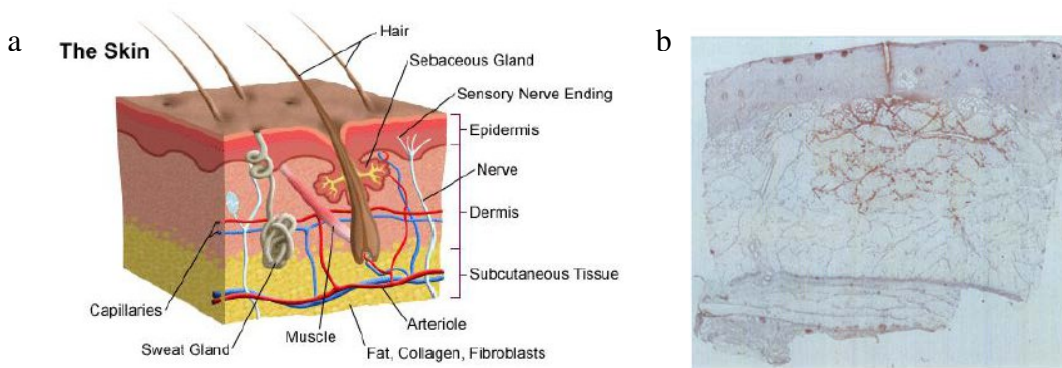


Figure 1. Structure of the human skin [4](a) and histology of an insulin depot from injection performed in pig tissue (b).

Insulin is injected in the subcutaneous tissue where it forms a depot, seen from the histology slice in figure 1b. The insulin diffuses from the injection site to the blood vessels, which makes the injection more long acting then compared to injecting directly to the blood vessels.

Measuring the level of radioactivity on the injection site as function of time gives information about the absorption. These kinds of measurements have been compared to the blood sugar level and correlation between the absorption and blood sugar level has been observed [5]. The absorption rate and insulin plasma concentrations measured have expressed large fluctuations, both from patient to patient and from injection to injection in the same patient ([6], [5]). This variation is illustrated in figure 2, which shows the insulin plasma concentration for 42 healthy persons after an injection of 0.4 U/kg NPH insulin [7]

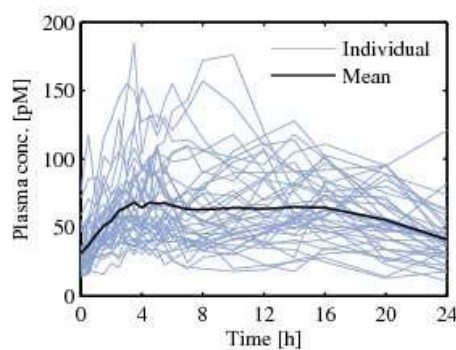


Figure 2. Insulin plasma concentration for 42 healthy person after injection of NPH insulin [7].

2. X-ray absorption tomography

Adding an iodine based contrast agent to the insulin the injection depot in the small samples of pork tissue can be visualized by μ CT. Compared to previously studies with PET and histology, μ CT make is possible to obtain information about the variation in the 3 dimensional structure of the depot.

2.1 Experimental setup

The experiments are performed at Department of Physics, The Technical University of München at a rotating anode with a Molybdenum target. The beam has been blended with a 2 mm Aluminium filter to reduce the effect of beam hardening and avoid the detector from being saturated. The maximum acceleration voltage and current for this setup was 50 kV and 75 mA, which gives a flux around $2 \cdot 10^5$ counts/sec. The projection data were collected with a Pilatus 100K, which has a very low signal to noise ratio and read out of 40 ms. The combination of the high flux from the rotating anode and the fast read out time of the Pilatus a full tomography scan with 401 projections can be obtained in 44 sec. The experimental setup is shown in figure 3a and an example of a transmission image of an insulin injection is shown in figure 3b.

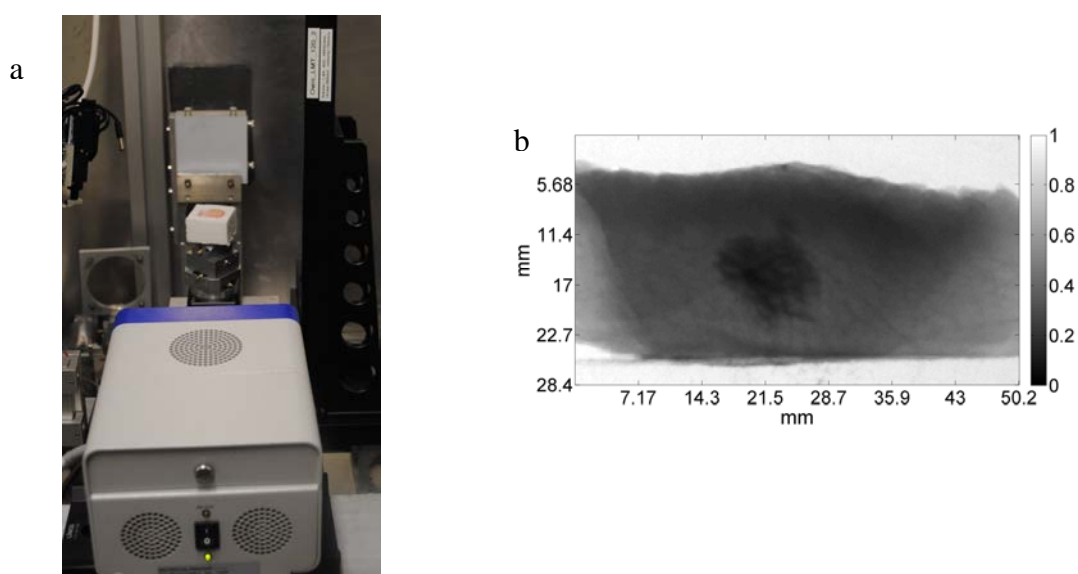


Figure 3. Experimental setup with a 2 mm Aluminium filter in front of the slit, the sample placed in a container of expanded polystyrene and the Pilatus detector (a). Transmission image of an injection of a dilution of insulin and an iodine based contrast agent (b)

1.2 Sample preparation

All the insulin injections were performed in tissue from the neck of the pig, shown in figure 4a. The fast acting insulin analogue Aspart U100 has been mixed with the contrast agent Xenetix 300 to a dilution of 8.4% of iodine. The injections are performed with a conventional insulin injection device.

Since the iodine is not labelled directly to the insulin molecules it is possible that the insulin and contrast agent spread differently in the tissue. We have made some comparison of the transmission images and histology slices and seen a good agreement between the distribution of insulin and iodine. For further validation we expect to compare results measured of some 0.2 mm thick slices at the x-ray tube directly compare them to histology made from the same slices.

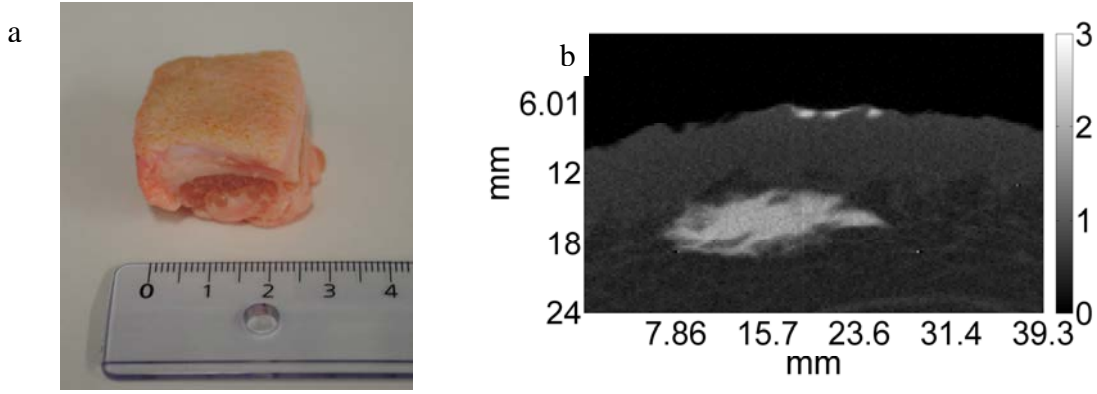


Figure 4. Neck tissue of pork before the injection (a). Slice of the 3 dimensional reconstruction of the injection depot(b)

1.3 Measurement and reconstructions

Just after the injection the samples were placed in a container of expanded polystyrene and a full tomography scan, with 401 projections with an exposure time of 70 ms for each projection, were made.

The reconstruction is performed by the filtered backprojection algorithm [8]. Since the distance from the source to the sample is 67.5 cm and the distance from source to the detector is 106.5 cm the rays from the source can be assumed to be parallel. A vertical slice of a reconstruction of a 0.1 ml injection is shown in figure 4b.

2. Data analysis

2.1 Segmentation

To avoid diffusion in the tissue during the measurement, the measuring time must be as short as possible, which means, that there is some noise in the reconstructions. Because of that, and because the iodine dilution become diluted in the tissue, it is not possible to make the segmentation by a normal threshold segmentation. Instead the Chan-Vese algorithm has been used. The Chan-Vese algorithm is an active contour model where an inertial contour, shown in figure 5a, is involved in time to find the minimum of the energy function given in equation (1) for the 2 dimensional case [9].

$$F(c^+, c^-, C) = \alpha \cdot \text{Length}(C) + \beta \int_{\text{inside}(C)} |u_0(x, y) - c^+|^2 dx dy + \beta \int_{\text{outside}(C)} |u_0(x, y) - c^-|^2 dx dy \quad (1)$$

where F is the energy function, u_0 is the image to be segmented and c^+ and c^- is the average value inside and outside the curve C respectively.

The curve that minimizes the energy function is the one with the shortest possible length that makes the region inside and outside the curve C as homogenous as possible. By selecting the weight of the two terms, expressed by α and β , correctly the final curve will fit the injection depot, which is illustrated in figure 5b for $\alpha=1$ and $\beta=6.7$.

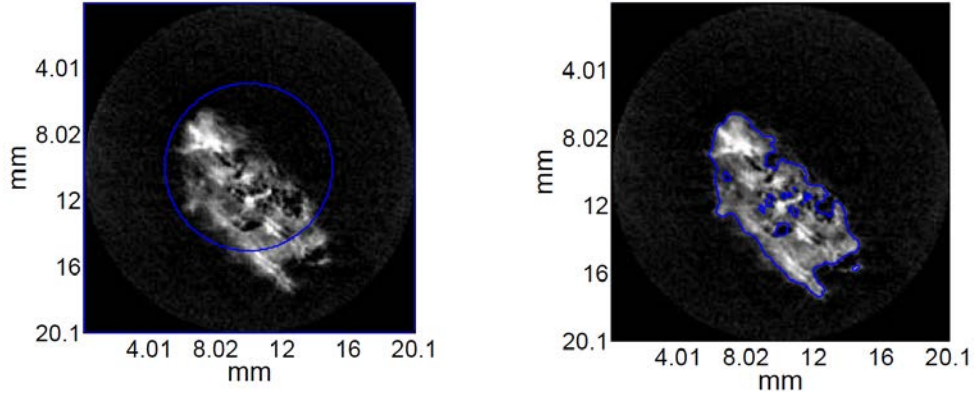


Figure 5. Inertial curve as input in for the Chan-Vese Algorithm (a). The final curve that minimize the energy function given in equation (1) (b).

When performing the injection, some of the injection fluid is pressed back though the injection channel and lay as a droplet on the top of the skin. This backflow has been segmented by threshold segmentation. Figure 6 shows an example of the 3 dimensional structure of an injection of 0.1 ml iodine dilution.

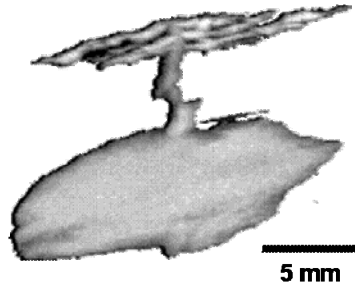


Figure 6. 3 dimensional structure of an injection depot for a 0.1 ml injection.

We have also measured on the samples at the μ CT Nanotom from phönix|x-ray, which has a normal anode. For the Molybdenum target the maximum acceleration voltage is 100 kV and the maximum current is 200 μ A, which means that the flux is much lower than at the rotating anode. The detector at the Nanotom has also a much higher signal-to-noise ratio, so the measuring time must be extended to 1½ hour for a single tomography scan. It means that the sample must be frozen during the measurement. The freezing process causes some deformation of the depot.

2.2 Surface area and volume

From the injection it is possible to calculate the surface area of the injection depot, excluding the backflow and the injection channel, by counting the pixels on the surface and find the volume filled by the injection depot by counting the number of segmented pixels.

What gives the contrast in absorption tomography is the absorption coefficient. In the segmented volume each voxel is a mixture of tissue and the iodine dilution given by equation (2) in the case of a monochromatic beam.

$$\mu = \epsilon\mu_{\text{dilution}} + (1 - \epsilon)\mu_{\text{tissue}} \quad (2)$$

where $\mu_{dilution}$ and μ_{tissue} is the absorption coefficient of the 8.4% iodine dilution injected and the tissue respectively. The absorption coefficient of the tissue will not be well defined due to the natural density variations in the skin.

The volume can be calculated by equation (3)

$$V = v_{voxel} \sum_i \frac{\mu - \mu_{tissue}}{\mu_{dilution} - \mu_{tissue}} \quad (3)$$

where v_{voxel} is the volume of a single voxel in the reconstruction and the sum runs over all voxels.

2.2.1 Beam hardening

For a polychromatic beam the transmission measured in a pixel at the point (s, ζ) on the detector is given by equation (4)

$$R_{\beta}(s, \zeta) = -\ln \left(\int_0^{\infty} W(E) e^{-\int_L \mu(E, x, y, z) dl} dE \right) \quad (4)$$

where $\mu(E, x, y, z)$ is the absorption coefficient at energy E for the point (x, y, z) in the sample and $W(E)$ is the ratio between the intensity of the beam at energy E and the total intensity.

In the reconstruction it is assumed that the transmission is given by [10]

$$R_{\beta}(s, \zeta) \approx \int_L \int_E W(E) \mu(E, x, y, z) dE dl \quad (5)$$

which only is a valid approximation for samples with a low absorption coefficient.

The approximation given by equation (5) causes some variation in the reconstructed absorption coefficient because the spectrum from the source change when penetration the sample. This effect is called beam hardening and is illustrated in figure 7a-b. It shows a slice of a plastic cylinder with a homogenous dilution of 30% Xenetix 300 and 70% Aspart U100 and a cylinder with pure water. It is seen from the figure that the beam hardening artefacts are most pronounced in the iodine dilution since the absorption coefficient is almost an order of magnitude higher then that of water.

These beam hardening artefacts makes it difficult to estimate the volume of the insulin injection, since the absorption coefficient in a single voxel do not only depend on the content of the iodine dilution and tissue, but also on the position of the voxel in the sample.

To be able to correct for the beam hardening artefacts we are working on making simulations by McXtrace, a Monte Carlo based simulation program. It has turned out that it is difficult to fit exact the measured result by the simulations, since the precise detector performance is hard to predict.

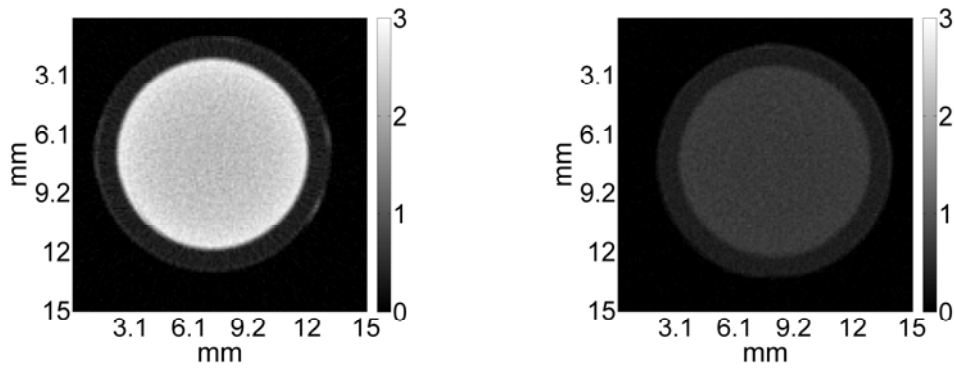


Figure 7. Variation in the reconstructed absorption coefficient for a cylinder with a homogenous dilution of 8.4% of iodine(a) and water(b).

2.4 Diffusion in death tissue

The short measuring time makes it possible to visualize the diffusion of the contrast agent in dead tissue. Figure 8 shows a single slice of a depot at time 0 and after 1½ hour and 4½ hour respectively.

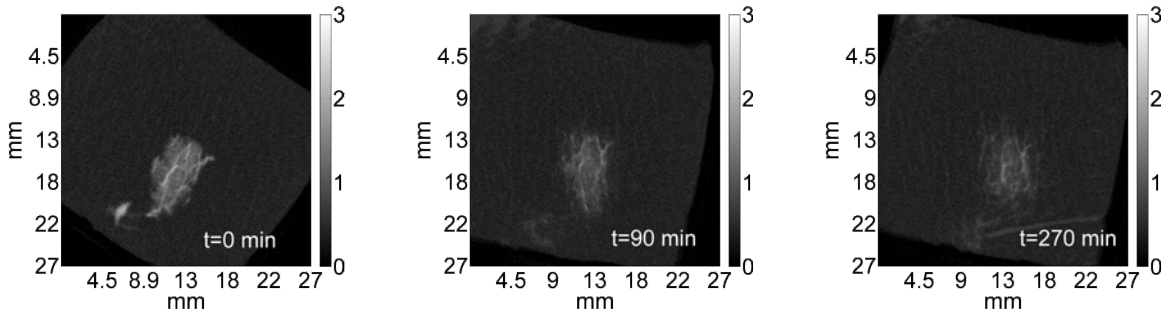


Figure 8. Diffusion of the contrast agent in dead pork tissue during a period of 4.5 hour.

The difference between same slice from tomograms obtained just after each other is very small so it can be assumed that the injection fluid not diffusion during a single measurement. Since only the diffusion of iodine can be visualized by μ CT the diffusion images must be compared to histology. This will be done by measuring a thin slice at a synchrotron and afterwards compare is it to histology. The reason for using synchrotron radiation is that the iodine has become very diluted during the 5 hours, and therefore it will be difficult to obtain any contrast at a laboratory source.

3. Conclusion

We have shown that it is possible to visualize the 3 dimensional structure of subcutaneous injections preformed in pig tissue in vitro, which not has been possible by the previous used techniques like PET and histology. To be able to measure on the injection depot the measurements must be preformed very fast to avoid diffusion during the scan. It means that a very high flux and a detector with a fast read out time and low signal to noise ratio is needed. To make the same measurements at a conventional x-ray tube, like Nanotom, it is necessary to freeze and keep the sample frozen during the measurement. The freezing process causes some deformation in the depot shape.

Computed tomography gives information about the volume distribution of iodine in the tissue, but due to beam hardening artefacts the volume can not be calculated by a simple

weighting of the absorption coefficient of each voxel. Therefore it is necessary to use simulations to reduce the variation of the absorption coefficient caused by beam hardening.

4. Outlook

The beam hardening artefacts can be avoided by performing measurements at a synchrotron source. The absorption coefficient of iodine decreases with increasing x-ray energy and has a discontinuity around 33 keV related to the binding energy of the k-electrons in the iodine atom. By using monochromatic radiation it is possible to compare tomograms measured at energies above and below k-edge and in that way improve the contrast of iodine. By this improved contrast it may also be possible to visualize insulin labelled directly with iodine.

Hopefully this method can be used as a tool for investigating the depot deformation and relate the shape to the composition of the tissue like density, thickness of subcutis, the elasticity of dermis, and to different injection parameters like injection speed, the geometry of the needle, the dose size and viscosity of the injection fluid.

The method can not only be used for in vitro injection, but also to measure on biopsies taken from testing animals after putting them down. These samples must be frozen to stabilize the injection from it is performed at the farm until the measurement. It means that the deformation both of the fluid and the tissue by the freezing must be characterized.

5. Acknowledge

We want to thank Franz Pfeiffer and his staff from Department of Physics, The Technical University of München for use of and help with the experimental setup. Specially we want to thank Astrid Velroyen and Martin Bech for help and advises during the experiments. Mads Nielsen and Jesper Rude Selknæs for introducing the segmentation algorithm and making the calculation run at the server.

6. References

- [1] Tim Holt & Subhesh Kumar. *Diabetes fra A-Z*. Wiley-Blackwell/BMJ-Books 2010
- [2] http://www.who.int/diabetes/facts/world_figures/en/
- [3] Rod R. Seeley Trent D. Stephens and Philip Tate. *Anatomy & Physiology*. McGraw-Hill, Higher Education, 2003, 6th ed.
- [4] University of Rochester Medical Center: Anatomy of the Skin. <http://www.urmc.rochester.edu/encyclopedia/content.cfm?pageid=P01336>
- [5] T. Lauritzen, O.K. Faber, C. Binder. *Variation in ^{125}I -Insulin Absorption and Blood Glucose Concentration*. *Diabetologia*, **1979**, 17, 291-295
- [6] Edward W. Moore et.al, *Variability in absorption of insulin- ^{131}I in normal and diabetic subjects after subcutaneous and intramuscular injection*, *J Clin Invest*. July 1959, 38(7): 1222–1227, July 1959.
- [7] T. Søbørg et.al, *Bioavailability and variability of biphasic insulin mixtures* (unpublished)
- [8] Avinash C. Kak & Malcolm Slaney. *Principles of Computed Tomography*. 1987
- [9] Tony F. Chan & Luminita A. Vese. *Active Contours Without Edges*. *IEEE Transactions on image processing*. 10, No. 2: 266-277. February 2001.
- [10] Chya Hwang Yan et al. *Reconstruction algorithm for polychromatic CT imaging. Application to beam hardening corrections*. *IEEE Transactions on medical imaging*, 19, No 1: 1-10, January 2000.